



# A mechanism for range image integration without image registration

Lyubomir Zagorchev & Ardeshir Goshtasby  
Department of Computer Science and Engineering  
Wright State University, Dayton, OH 45435  
{lzagorch, agoshtas}@cs.wright.edu

## Abstract

*A mechanism is introduced that automatically integrates multi-view range images without registering the images. The mechanism is based on a reference double-frame that acts as the coordinate system of the scene. A single-view range image of a scene is obtained by sweeping a laser line over the scene by hand and analyzing the acquired light stripes. Range images captured from different views of the scene will be in the coordinate system of the double-frame, and thus, will automatically integrate without further processing.*

## 1. Introduction

Determination of the 3-D geometry of a scene from its images is a fundamental problem in computer vision. Although 3-D information can be acquired through contact [15], one of the main objectives of computer vision is to acquire the same information through image analysis means. Methods for recovering 3-D geometry can be classified into passive and active. Passive methods, such as binocular stereo [26] or depth from defocus [28], use a scene's own lighting, while active techniques, such as structured light [19], Moiré interferometry [17], or time of flight [27] techniques use special lighting or signal to capture 3-D geometry. In this paper, the development of a range scanner based on the structured light principle is discussed.

In spite of more than three decades of research on range scanning techniques, work in this area actively continues. The main difficulty in range scanning is the registration of range images captured from different views. About one-third of all work on 3-D scanning appearing in recent conferences has been on the registration aspect of the problem [1, 2, 3, 4]. The idea proposed in this paper is to use a setup that does not require image registration for integrating multiple-view range images. One way to achieve this is to use multiple cameras that are in fixed positions of each other. A fixed camera setup will make it possible to trans-

form one camera coordinate system to another camera coordinate system and combine range images captured from different cameras into the coordinate system of one of the cameras or into a standard coordinate system. Examples of such scanners are the Cyberware whole-body scanners [6].

An alternative approach is to use a coordinate system that is attached to the scene to determine the coordinates of points in the scene with respect to that coordinate system rather than with respect to the coordinate system of the camera. In [13], various fiducials that act as the coordinate system of the scene were introduced. In this paper, a double-frame geometry is introduced that acts as the scene's coordinate system and allows the capture of range images from different views and automatic integration of the images without image registration. By sensing the intersections of the laser sheet with the frame borders, the equation of the laser plane is determined, and by locating distinctly marked frame corners in images, the position and orientation of the camera is determined. This mechanism allows the laser and the camera to be moved independently while scanning the scene. Captured scene points will always be in the coordinate system of the scene and, therefore, will automatically come together to reconstruct the scene.

In the following sections, first, a brief review of existing laser scanning methods is made. Then, the organization of the proposed scanner is described. Next, the speed and accuracy of the scanner are determined, and finally, example scans obtained by the scanner are provided.

## 2. Related Work

Depth from binocular stereo is perhaps the most natural way of capturing 3-D information about a scene. Binocular stereo, however, depends heavily on a correspondence process that easily fails when the scene is textureless. As a means to add texture to the scene, light stripes and light grids have been used. Hérbert swept the scene with a laser crosshair while capturing and analyzing the images of the crosshair [14]. Davis and Chen simplified the stereo setup by using a single camera but using a hinged mirror that cap-

tured left and right view images simultaneously [7]. Use of a hinged mirror and a single camera simplifies stereo calibration and rectifies the images [12].

From the desire to construct a hand-held scanner, McCallum et al. [18] positioned a laser line generator between two cameras in a scanner head. The head was equipped with a magnetic tracker that determined the position and orientation of the head at any instant. Range data captured with respect to the scanner head was then transformed into a global coordinate system. Based on the same principle but using a single camera, a hand-held scanner was developed by Ferreira et al. [10]. A laser source and a camera are sufficient to capture 3-D. In a system developed by Strat and Oliveira [25], a rotating mirror and circuitry to turn the laser source on and off with fast speed were used. As the laser is swept over a scene with a rotating mirror, the laser is turned on and off in high speed creating a set of equally spaced laser stripes in the same image frame. This setup makes it possible to produce a single-view range image of a scene from a single camera shot.

Image registration algorithms have become more elaborate throughout years of research. They can currently combine tens and even hundreds of range images into a single 3-D model [21]. Range image registration algorithms can be categorized into those that work with image features and those that work with raw range values. Examples of features are ridge curves [20] and local peak points in single-view range images [8]. Matching of range features is achieved through subgraph isomorphism [9]. Ramalingam and Lodha [22] registered range images using point features obtained by a corner detector. They then refined the registration using all range points in an iterative closest point (ICP) algorithm [5]. Typically, in an ICP algorithm, for each range point in one image, the closest range point in another image is found and the sum of such distances is used as the match rating. One surface is slid over the other by incrementally changing the translation and rotation parameters in the gradient-descent direction of the sum of distances until the process converges.

Many registration algorithms have offered improvements to the original ICP algorithm [5]. Steps have been taken to make the ICP algorithm faster and more resistant to outliers. To speed up the ICP algorithm, coarse-to-fine approaches have been proposed by Jost and Hugli [16] and Schonfeld et al. [23]. To improve the geometric stability of the ICP algorithm, Gelfand et al. [11] devised a point selection strategy that samples those points in the input that provided the best convergence of the algorithm to the correct pose. The sampling strategy estimated the transformation that produced unstable sliding of one surface over another and picked those points that best constrained this sliding. To avoid convergence to a local minimum, Silva et al. [24] searched in the parameter space for the best-match position

with a genetic algorithm. Contrary to the ICP algorithm, a genetic algorithm does not require pre-alignment of the images.

In spite of all these advancements, image registration still remains a major hurdle in 3-D data acquisition. If overlap between views is small, there is no guarantee that a registration method can correctly integrate the images. A scanner mechanism is introduced in this paper that does not require image registration to integrate multi-view range images. The scanner measures all range values with respect to a coordinate system that is attached to the scene. The camera and the laser source can be moved around the scene obtaining multi-view range images and the images automatically come together to reconstruct the scene.

### 3. Organization of the scanner

#### 3.1. Hardware organization

The hardware organization of the scanner is shown in Figure 1. Figure 1a shows the structure of a reference double-frame.  $W$  and  $H$  are, respectively, the width and height of the front frame;  $w$  and  $h$  are the width and height of the back frame; and  $d_x$ ,  $d_y$ , and  $d_z$  are distances between the lower-left corners of the front and back frames along the  $x$ ,  $y$ , and  $z$  axes, respectively. Figure 1b shows the relation between the camera, the laser plane, and the double-frame. Scanning is done by sweeping the laser light over an object by hand, just like painting the object with a paintbrush.

The world coordinate system is attached to the double-frame, and as long as the position of the object remains fixed with respect to the double-frame, object coordinates determined from different views will automatically merge to produce a larger data set that represents a more complete view of the scene. The scanner, therefore, makes it possible to combine different-view range images of a scene without registering the images. Another characteristic of the scanner is that the camera and the laser source need not be fixed with respect to each other, and the user can move the laser independent of the camera during a scan.

#### 3.2. Software organization

As the laser light is swept over a scene, the images captured by the camera are processed to obtain the 3-D coordinates of scene points along the light stripes. If camera lens distortions can be considered negligible, the relation between points in the front frame and their images can be written by a projective transformation:

$$X_f = \frac{a_1x + a_2y + a_3}{a_4x + a_5y + 1}, \quad (1)$$

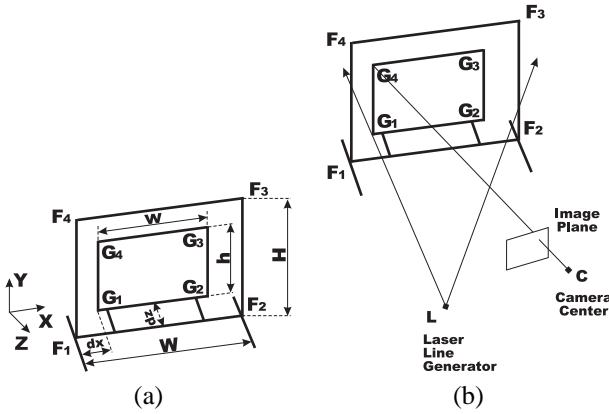


**Figure 1. (a) The structure of the reference double-frame. (b) Relation between the camera, the laser light, and the double-frame.**



**Figure 2. The actual double-frame during a scan.**

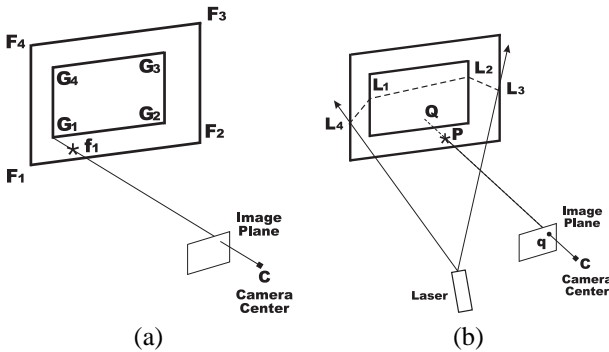


**Figure 3. (a) The relation between the camera (lens) center and the front and back frames. (b) Finding the coordinates of an object point in 3-D from the coordinates of its image.**

$$Y_f = \frac{a_6x + a_7y + a_8}{a_4x + a_5y + 1}. \quad (2)$$

$(X_f, Y_f)$  are coordinates of points in the front frame,  $(x, y)$  are coordinates of corresponding points in the image plane, and  $a_1-a_8$  are the parameters of the transformation. The  $XY$ -plane is taken to be the plane of the front frame and the origin is taken to be the lower-left corner of the front frame. Knowing the coordinates of the four corners of the front frame and their images, parameters  $a_1-a_8$  are determined by solving a system of linear equations. The relation between points in the back frame and their images can be determined similarly.

During a normal scan, the plane of laser intersects two of the borders in each frame. Assuming the intersections of the laser plane with the back frame are  $L_1$  and  $L_2$  and with the front frame are  $L_3$  and  $L_4$ , by determining the images of these four intersections, their 3-D coordinates can be determined. The equation of the laser plane can be written as:

$$Z = AX + BY + C, \quad (3)$$

parameters  $A, B, C$  can be determined using the coordinates of the intersections of the laser plane with the front and back frames by the least-squares method. To determine the intersection of the laser sheet with the left or right frame border, the laser point on the frame border that has the same  $X$  coordinate as the top or bottom marker is used, and to determine the intersection of the laser sheet with the top or bottom border in a frame, the laser point having the same  $Y$  coordinate as that for the left or right marker is used.

If the plane of laser intersects the front or the back frame at only one point due to occlusion by the object, rather than using the least-squares method, the parameters of the plane are obtained by solving a system of three linear equations. If the laser plane does not intersect one of the frames, the equation of the laser plane cannot be determined and so range data cannot be acquired.

From the preceding discussions, it can be concluded that each point in the image plane corresponds to a point in the front frame and a point in the back frame. The two points lie on a ray that passes through the lens center. Figure 3a shows this situation. Let's suppose the line connecting the lens center to the lower left corner of the back frame (point  $G_1$ ) intersects the front frame at  $f_1$ . The coordinates of the lens center (point  $C$ ) is not known, but the coordinates of  $G_1$  in 3-D is known, and the coordinates of  $f_1$  can be determined. Similarly, the rays that connect points  $G_2, G_3,$  and  $G_4$  to their images can be determined. All these rays should pass through the lens center. Theoretically, by the intersection of any two such rays, it should be possible to determine the position of the lens center. But because of the discrete nature of the images, the lines may not intersect. They will, however, pass close to each other near the lens center.

To determine the position of the lens center, the point in 3-D whose sum of squared distances to the four rays is minimum is computed. Assuming the 3-D coordinates of points  $G_1$  and  $f_1$  are  $\mathbf{P}_1$  and  $\mathbf{P}'_1$ , respectively, the parametric line passing through them can be written as:

$$\mathbf{P} = \mathbf{P}_1 + (\mathbf{P}'_1 - \mathbf{P}_1)t. \quad (4)$$

Assuming  $\mathbf{P}_c$  shows the lens center, the distance of the lens center to the point with parameter  $t$  on the line is

$$d^2 = \|\mathbf{P}_1 + (\mathbf{P}'_1 - \mathbf{P}_1)t - \mathbf{P}_c\|^2. \quad (5)$$

The value of  $t$  that minimizes  $d^2$  can be determined by finding the derivative of  $d^2$  with respect to  $t$ , setting it to zero, and solving the obtained equation. Denoting the obtained parameter by  $t_1$ , we have

$$t_1 = \frac{-(\mathbf{P}_1 - \mathbf{P}_c)(\mathbf{P}'_1 - \mathbf{P}_1)}{(\mathbf{P}'_1 - \mathbf{P}_1)^2}. \quad (6)$$

Similarly, rays connecting  $G_2, G_3$ , and  $G_4$  to their images can be determined and the point on each ray closest to  $\mathbf{P}_c$  can be computed. Suppose the closest points on the three rays have parameter coordinates  $t_2, t_3$ , and  $t_4$ . Using equation (5), the sum of squared distances of point  $\mathbf{P}_c$  to the four rays can then be written as

$$E^2 = \sum_{i=1}^4 \|\mathbf{P}_i + (\mathbf{P}'_i - \mathbf{P}_i)t_i - \mathbf{P}_c\|^2. \quad (7)$$

Substituting  $t_1 - t_4$  into equation (7),  $E^2$  will be in terms of  $\mathbf{P}_c$ . To determine  $\mathbf{P}_c$  that minimizes  $E^2$ , partial derivatives of  $E^2$  with respect to  $X_c, Y_c$ , and  $Z_c$  are obtained and set to zero and the three linear equations are solved for  $X_c, Y_c$ , and  $Z_c$ . The lens center obtained in this manner will be the average of the lens centers estimated by the four rays.

To determine the coordinates of object points, supposing the image of an object point  $\mathbf{P}$  is point  $\mathbf{q}$  in the image plane as shown in Figure 3b. Point  $\mathbf{q}$  also corresponds to a point in the back frame. Let's call that point  $\mathbf{Q}$ . The coordinates of  $\mathbf{Q}$  can be determined using the coordinates of  $\mathbf{q}$ . The equation of the laser plane can also be determined from the coordinates of the intersections of the laser plane with the front and back frames. Knowing the coordinates of the lens center  $\mathbf{C}$  and the coordinates of point  $\mathbf{Q}$ , the intersection of the ray passing through points  $\mathbf{C}$  and  $\mathbf{Q}$  and the laser plane produces the coordinates of the object.

Missing points due to self occlusion can often be recovered by scanning the scene from a different view. Missing data due to the dark color of an object, however, may not be recoverable by rescanning. The solution we propose is to fit a surface to the points and let the surface fill in the missing points. We will use a weighted mean approach to achieve

this. A weighted mean surface that approximates  $N$  irregularly spaced points in 3-D  $\{\mathbf{V}_i : i = 1, \dots, N\}$  is defined by

$$\mathbf{P}(u, v) = \frac{\sum_{i=1}^N W_i(u, v)\mathbf{V}_i}{\sum_{i=1}^N W_i(u, v)} \quad u, v \in [0, 1], \quad (8)$$

where  $W_i(u, v)$  is the  $i$ th weight function of the surface and is defined by

$$W_i(u, v) = \{(u - u_i)^2 + (v - v_i)^2 + \delta\}^{-\frac{1}{2}}, \quad (9)$$

which is the inverse distance between the surface point under consideration and a data point.  $\delta$  is a small number to ensure that the weights do not become undefined at the data points.  $(u_i, v_i)$  are the parameter coordinates associated with the  $i$  point, showing the relation of that point with respect other points in the scene. If a range data set represents a single view of an object, the surface to be constructed is single valued, and  $(u_i, v_i)$  may be set proportional to  $(X_i, Y_i)$ . If a range image represents a cylindrical scan of an object,  $u$  may be used to show the height of the cylinder and  $v$  may be used to show the rotational angle in each circular cross-section of the cylinder. The weighted mean surface will not only fill in areas where data are missing, it will reduce data in areas where multiple range values are available, smooth digital noise among the points, and generate a regular grid of points for rendering purposes.

It is often necessary to map the natural texture of a scanned object to the reconstructed object to give it a realistic appearance. For texture mapping, the correspondence between object coordinates and texture coordinates should be established. This is straightforward when mapping the texture from a single view of an object to the reconstructed surface. In many situations, however, there is a need to map texture from different views of an object to the reconstructed object. This is achieved by first determining the texture coordinates for each recovered 3-D point. In this way, at each point on the reconstructed surface there will be not only the  $X, Y$ , and  $Z$  coordinates of the point but also the  $R, G, B$  color of the point. Therefore, instead of fitting a surface with three components to the obtained range data, a surface with six components is fitted to the range and texture data. By varying  $u$  and  $v$  from 0 to 1, the surface is generated using the first three components of the surface and its texture is determined using the last three components of the surface. This process will not only fill in missing range values, it will fill in missing texture values also. Texture in an overlap area is the average of textures from the views covering the area.

In our setup a red laser is used, therefore, only the red channel from a video sequence is processed to locate the laser stripe. To detect a point along the spine of a laser

stripe, the red component of an image frame is smoothed with a Gaussian to reduce image noise. The size of the Gaussian smoother depends on the amount of noise in the image and can be determined experimentally. Next, the smoothed image is thresholded. The threshold value depends on the intensity of the laser and the environment lighting. This is also determined through experimentation. The thresholding process separates the laser stripe from the background in an image and reduces the search space for determining the spine of the stripe. To locate the spine with subpixel positional accuracy, a biquadratic function is fitted to  $3 \times 3$  neighborhoods centered at locally maximum intensities within a stripe and the peak of the fitting function is traced.

#### 4. Resolution and accuracy of the scanner

The resolution in  $X$  and  $Y$  directions is determined by the size of pixels in an image. If an image pixel covers a 1 mm by 1 mm area in the scene, resolutions in  $X$  and  $Y$  directions will be 1 pixel/mm. To determine the resolution in  $Z$  direction, a translation stage is used. Suppose a horizontal laser stripe on a vertical plane that is parallel to the image plane falls on scanline  $h_1$ . If after moving the plane  $d$  mm parallel to itself the horizontal stripe shifts to scanline  $h_2$ , the resolution of the scanner in  $Z$  direction will be  $(h_2 - h_1)/d$  pixels/mm.

To determine the accuracy of the scanner in practice, an Egyptian art piece as shown in Figure 4a was used. The width of the portion of the plaque shown here is 312 pixels. These 312 pixels corresponded to 161 mm on the plaque. Therefore, the resolution of the scanner along a scanline is  $161/312$  or about 0.52 mm. To determine the accuracy of the scanner in  $Z$  direction, the actual difference between the highest point on the plaque and the lowest point on the plaque was estimated manually with a ruler. This difference was estimated to be less than 3 mm. The plaque was then scanned with the triangulation angle in the range of 75–90 degrees and the depths of points on the plaque were determined. Seven discrete depth values were obtained over the plaque. Therefore, the obtained resolution along the  $Z$  axis is  $3/7$  or 0.43 mm. Further accuracy in depth can be achieved by either zooming in and scanning a smaller scene area or using a higher resolution camera. Isovalued depth contours with 0.43 mm spacing are shown in Figure 4b. A uniform B-spline surface fitting to the range data is shown in Figure 4c. Details in the geometry of the plaque that were not even visible in the plaque intensity image have become visible. The surface fitting process has smoothed digital noise in estimated depth values and has restored the smooth geometry of the plaque.

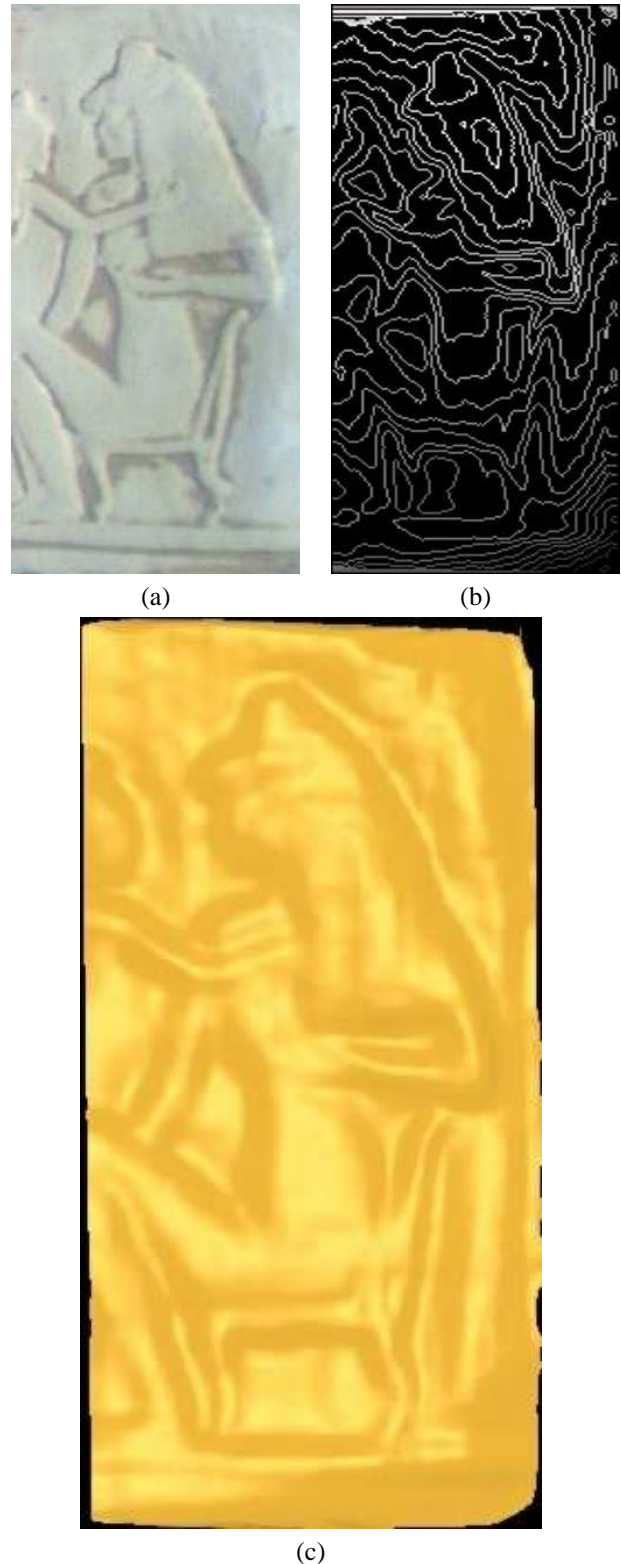


**Figure 4. (a) An image of an Egyptian plaque. (b) Isovalued depth contours of the plaque with 0.43 mm spacing. (c) B-spline surface approximation of the range data.**

## 5. Example scans

Different examples of scans produced by the scanner are presented in this section. In the first example, a model of a human face was reconstructed from two separate laser positions but with the same camera view. Figure 5 shows the model of the human face that was placed between the front and back frames. In the first scan, the range data set shown in Figures 6a-c was obtained by sweeping the laser from the left side. The range data set shown in Figure 6d-f was acquired by sweeping the laser from the right side. As can be observed, gaps are obtained in areas where the laser is not visible to the camera due to self occlusion of the object. The size of such gaps depends on the position of the laser, the position of the camera, and the geometry of the object. Combining the range data sets captured from the two different views of the laser source and filling in the gaps by the weighted mean method produces the range data set shown in Figures 6g-i. A non-uniform B-spline surface fitted to the range points is shown in Figures 7a-c. The figures show a smooth reconstruction of the model face by a B-spline surface. The reconstructed model after mapping the acquired texture to it is shown in Figures 7d-f. The images of the texture-mapped reconstructed face model are almost indistinguishable from those of the actual model face.

In the next example, a Greek statue as shown in Figure 8 was scanned from two camera views. The scan from the left camera view produced the range data set shown in Figures 9a-c and the scan from the right view of the camera produced the range data set shown in Figures 9d-f. After integrating the two data sets by finding the union of the 3-D points, the combined range data set shown in Figures 9g-i was obtained. The overlap between the two scans is not large but the scans are large enough to cover the entire front, left, and right sides of the statue. A B-spline surface fitting to the integrated data is shown in Figures 9j-l. As can be observed, the surface is smooth and seamless at places where different-view range images overlap and merge. The texture mapped surface is shown in Figures 9m-o.

## 6. Summary and conclusions

A scanning mechanism was introduced that makes it possible to capture range data from different views of an object and integrate the data without image registration. Based on this mechanism, the design of a portable low-cost laser range scanner was described that has the ability to scan an object with adjustable density and accuracy. The scanner does not require that the laser source and the camera be fixed with respect to each other. The user may hold the laser line generator in hand and sweep over an object to scan it while keeping the camera stationary. The camera can then be moved and the process can be repeated to obtain

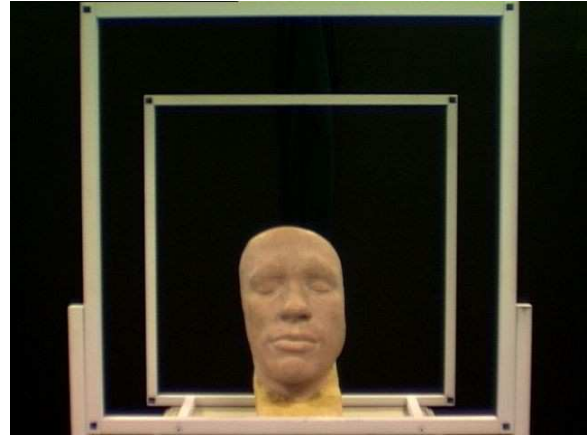


Figure 5. A face model used in the experiments.

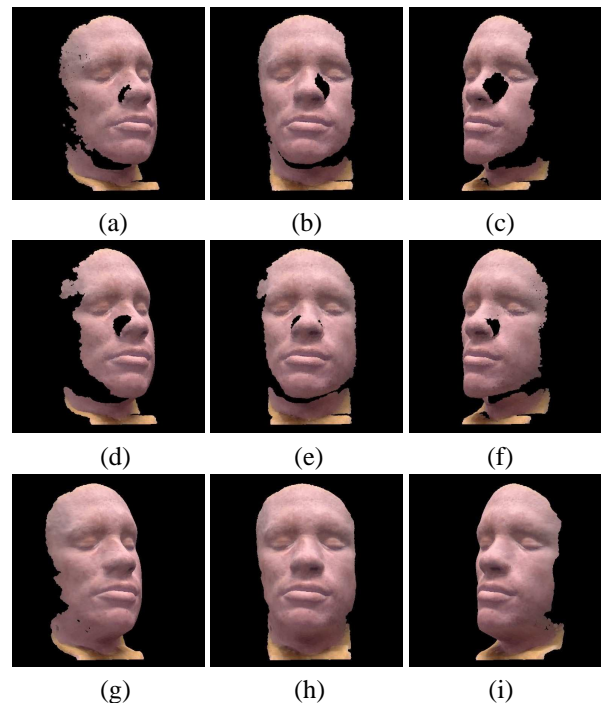
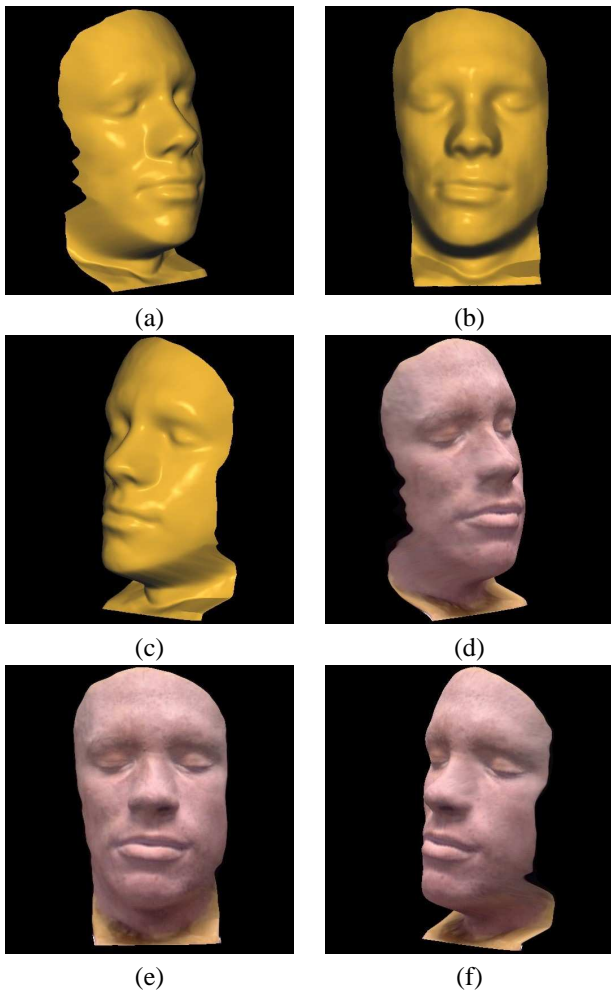


Figure 6. (a)-(c) Three views of the range data captured by sweeping the laser from the left side. (d)-(f) Three views of the range data captured by sweeping the laser from the right side. Both scans were obtained at the same camera position and orientation. (g)-(i) Three views of the data obtained by integrating the two laser scans and filling the holes in the image space. Some small holes still appear in data when viewed from the side



**Figure 7. (a)-(c) Three views of the B-spline surface approximating the combined range data set shown in Figs. 6g-i. (d)-(f) Views of the reconstructed model face after texture mapping.**



**Figure 8. (a) Left view of the Greek statue. (b) Right view of the statue.**

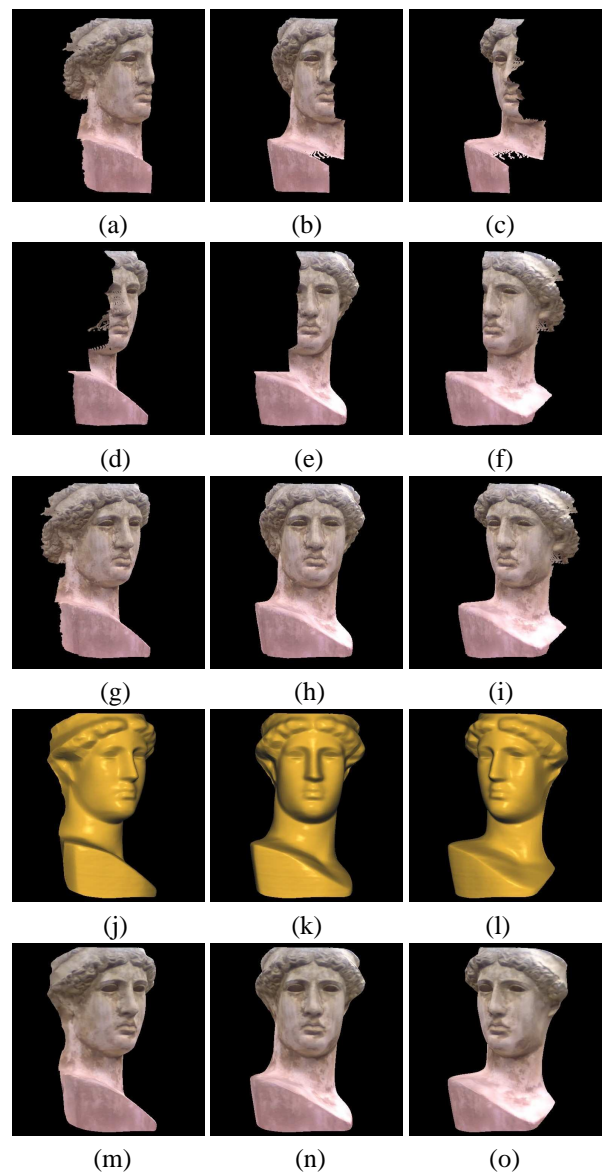


**Figure 9. (a)-(c) Three views of the range data set obtained when scanning the statue while the camera viewing the statue from the left. (d)-(f) Views of the range data set when the camera viewing from the right. (g)-(i) Views of the integrated data set. (j)-(l) Views of the reconstruct statue geometry by fitting a B-spline surface to the combined range data. (m)-(o) Views of the reconstructed statue in texture mapped form.**

different-view images of the object. Range data captured from different views of the object will be in the coordinate system of a reference frame that is fixed with respect to the object and is visible in all images. With this mechanism it is possible to automatically integrate range data captured from different views of an object and create a model of the object. Depending on the size of the scanned area and the angle between the laser and camera directions, varying accuracy in captured range values can be achieved. Sub-millimeter accuracy in depth can be achieved if the scanned area is 20 square cm or smaller, the angle between the laser and the camera axis is at least 60 degrees, and captured images are of size  $640 \times 480$  pixels or larger.

## References

- [1] 3DICA. *Three-Dimensional Image Capture and Applications*. Proc. SPIE, San Jose, CA, January 27–29 1998.
- [2] 3DIM. *Proc. 1st Int'l Conf. 3-D Digital Imaging and Modeling*. Ottawa, Canada, Oct. 4–8 1999.
- [3] 3DIM. *Proc. 4th Int'l Conf. 3-D Digital Imaging and Modeling*. Banff, Alberta, Canada, Oct. 6–10 2003.
- [4] 3DPVT. *Proc. 1st Int'l Sym. 3-D Data Processing Visualization and Transmission*. Padova, Italy, June 19–21 2002.
- [5] P. J. Besl and N. D. McKay. A method for registration of 3-d shapes. *IEEE Trans. Pattern Analysis and Machine Intelligence*, 99(7):239–256, January 1992.
- [6] Cyberware. <http://www.cyberware.com/>.
- [7] J. Davis and X. Chen. A laser range scanner designed for minimum calibration complexity. *Proc. 3rd Int'l Conf. 3-D Digital Imaging and Modeling*, 2001.
- [8] F. DePiero. Fast landmark-based registration via deterministic and efficient processing, some preliminary results. *Proc. 1st Int'l Sym. 3-D Data Processing Visualization and Transmission*, pages 544–548, June 19–21 2002.
- [9] F. W. DePiero, M. M. Trivedi, and S. Serbin. Graph matching using a direct classification of node attendance. *Pattern Recognition*, 29(6):1031–1048, 1996.
- [10] J. Ferreira, J. Lobo, and J. Dias. Tele-3d – developing a handheld scanner using structured light projection. *3-D Data Processing, Visualization and Transmission*, 2002.
- [11] N. Gelfand, L. Ikemoto, S. Rusinkiewicz, and M. Levoy. Geometrically stable sampling for the icp algorithm. *Proc. 4th Int'l Conf. 3-D Digital Imaging and Modeling*, pages 260–267, Oct. 6–10 2003.
- [12] A. Goshtasby. Design and recovery of 2-d and 3-d shapes using rational gaussian curves and surfaces. *Int'l J. Computer Vision*, 10(3):242–263, 1993.
- [13] A. Goshtasby, S. Nambala, W. deRijk, and S. Campbell. A system for digital reconstruction of gypsum dental casts. *IEEE Trans. Medical Imaging*, 16(5):664–674, 1997.
- [14] P. Hébert. A self-referenced hand-held range scanner. *Proc. Int'l Conf. Recent Advances in 3-D Digital Imaging and Modeling*, pages 5–12, 2001.
- [15] R. Howe and M. Cutkosky. Dynamic tactile sensing: Perception of fine surface features with stress rate sensing. *IEEE Trans. Robotics and Automation*, pages 140–151, 1993.
- [16] T. Jost and H. Hugli. A multi-resolution icp with heuristic closest point search for fast and robust 3-d registration of range images. *Proc. 4th Int'l Conf. 3-D Digital Imaging and Modeling*, pages 427–433, Oct. 6–10 2003.
- [17] G. G. Levin, G. N. Vishnyakov, A. A. Naumov, and S. S. Abramov. 3-d surface real-time measurement using phase-shifted interference fringe technique for the craniofacial identification. *3-D Image Capture and Applications, Proc. SPIE*, January 1998.
- [18] B. McCallum, M. Nixon, B. Price, and R. Fright. Hand-held laser scanning in practice. *Proc. Image and Vision Computing*, pages 17–22, Oct. 1998 1998.
- [19] J. Mundy and G. Porter. A three-dimensional sensor based on structured light. *Three Dimensional Machine Vision*, pages 3–61, 1987.
- [20] X. Pennec, N. Ayache, and J.-P. Thirion. Landmark-based registration using features identified through differential geometry. *Handbook of Medical Imaging*, pages 499–513, Sept. 2000.
- [21] K. Pulli. Multiview registration for large data sets. *Proc. 2nd Int'l Conf. 3-D Digital Imaging and Modeling*, pages 160–168, Oct. 4–8 1999.
- [22] S. Ramalingam and S. K. Lodha. Adaptive enhancement of 3-d scenes using hierarchical registration of texture-mapped 3-d models. *Proc. 2nd Int'l Conf. 3-D Digital Imaging and Modeling*, pages 203–210, Oct. 4–8 1999.
- [23] H. Schonfeld, G. Häusler, and S. Karbacher. Reverse engineering using optical 3-d sensors. *3-D Image Capture and Applications, Proc. SPIE*, January 1998.
- [24] L. Silva, O. R. P. Bellon, and K. L. Boyer. Enhanced, robust genetic algorithms for multiview range image registration. *Proc. 4th Int'l Conf. 3-D Digital Imaging and Modeling*, pages 268–275, Oct. 6–10 2003.
- [25] A. V. Strat and M. M. Oliveira. A point-and-shoot color 3-d camera. *Proc. 4th Int'l Conf. 3-D Digital Imaging and Modeling*, Oct. 6–10 2003.
- [26] E. Trucco and A. Verri. *Introductory Techniques for 3-D Computer Vision*. Prentice-Hall, New Jersey, 1998.
- [27] A. Ullrich, N. Studnicka, and J. Riegl. Long-range high-performance time-of-flight based 3-d imaging sensors. *Proc. 1st Int'l Sym. 3-D Data Processing Visualization and Transmission*, pages 852–855, June 19–21 2002.
- [28] M. Watanabe and S. Nayar. Rational filters for passive depth from defocus. *Int'l J. Computer Vision*, 23(3):203–225, 1998.